

K. Arikawa · H. Uchiyama

Red receptors dominate the proximal tier of the retina in the butterfly *Papilio xuthus*

Accepted: 8 June 1995

Abstract 1. The ommatidia of the butterfly *Papilio* have a fused and tiered rhabdom. The distal tier of the rhabdom is made up of four distal photoreceptors (R1-4), whereas the proximal tier is made up of four proximal (R5-8) and one basal photoreceptor cell (R9). 2. We first confirmed by light microscopy that the ommatidia of *Papilio* are not twisted, i.e. have the same spatial organization all about the longitudinal axis. The polarization method, previously applied to the distal tier, hence is applicable to identify the photoreceptor location from the peak angle of the polarization sensitivity. 3. We determined the polarization and spectral sensitivity of in total 109 proximal and basal photoreceptors in the lateral looking eye region. All of the photoreceptors were either green or red type, most of which fall into three classes as judged by the peak angles of the polarization sensitivity: around 40°, 150°, and 180° (= 0°) with respect to the dorso-ventral axis. The first two classes are formed by the proximal photoreceptors with straight microvilli oriented at the average angle of 39° (R6, 8) and 144° (R5, 7) respectively, and the third is formed by the basal photoreceptors R9 with straight microvilli oriented at 180° (= 0°). The mean polarization sensitivity (PS = maximal sensitivity/minimal sensitivity) was about 2. 4. 75% of the proximal and 48% of the basal photoreceptors were of the red type. 5. A single ommatidium of *Papilio* appears to contain two to four types of spectral receptors.

Key words Electrophysiology · Lepidoptera · Photoreceptor · Spectral sensitivity · Vision

Introduction

Colocalization of photoreceptors with different spectral sensitivity in the retina is a fundamental requirement for color vision. Color vision has been conclusively demonstrated only in primates and honeybees as a trichromatic system whose chromatic units correspond to the spectral sensitivities of retinal photoreceptors (Goldsmith 1990). However, many vertebrates have four types of spectral receptors, while the compound eyes of some arthropods are furnished with at least five (butterfly *Papilio*, Arikawa et al. 1987; butterfly *Pieris*, Shimohigashi and Tominaga 1991; dragonfly *Hemicordulia*, Yang and Osorio 1991) or even ten types of spectral receptors (mantis shrimp *Pseudosquilla*, Cronin and Marshall 1989). Do these animals have a color vision system based on more than four chromatic units? The localization pattern of the spectral receptors in the retina would serve as a good starting point to address this question.

The subject of this study, the Japanese yellow swallowtail butterfly, *Papilio xuthus*, was shown to have five types of spectral receptors in the compound eye (Arikawa et al. 1987). The ommatidium of *Papilio* is of the apposition type with a fused and tiered rhabdom. The rhabdomeres of four photoreceptors (R1-4) together constitute the distal tier of the rhabdom, while the proximal rhabdom is made up by rhabdomeres of five other photoreceptors (R5-9). The rhabdomere of the ninth photoreceptor (R9) is restricted to the very basal part of the rhabdom (Bandai et al. 1992; Ribi 1987). As the ommatidium contains more than two different types of spectral receptors, there is the potential for simultaneous analysis of different spectral bands. We previously compared the spectral and polarization sensitivities of photoreceptors and revealed that R1 and R2 were either UV, violet, or blue receptors, whereas R3 and R4 were all green type (Bandai et al. 1992). By applying the same procedures to the proximal

K. Arikawa (✉) · H. Uchiyama
Department of Biology, Yokohama City University,
22-2 Seto, Kanazawa-ku, Yokohama 236, Japan

tier of the rhabdom we here determined the spectral properties of the proximal and basal photoreceptors.

Materials and methods

Animals

We used the spring form of the Japanese yellow swallowtail butterfly, *Papilio xuthus*, within 3 days after emergence. The butterflies were reared on fresh citrus leaves throughout the larval stage at 25°C under a light regime of 8 h light : 16 h dark. The pupae were stored at 4°C for at least 2 months, and then allowed to emerge at 25°C.

Anatomy

For light and electron microscopy, the compound eyes were prefixed with 2% glutaraldehyde and 2% paraformaldehyde in 0.1 M sodium cacodylate buffer (pH 7.4) at 4 °C for 12 hs, and post-fixed with 2% OsO₄ in the same buffer at room temperature for 2 hs. Tissues were then dehydrated in an ethanol series and embedded in Epon. Semithin sections were stained with toluidine blue. Ultrathin sections were double stained with uranyl acetate and lead citrate.

Electrophysiology

A butterfly was mounted in a Faraday cage and the eye's vertical axis, which was determined by observing the hexagonal reflection pattern on the eye surface, was adjusted to a reference pendulum set in the cage. A hole covering about 10 to 20 facets was made in the dorsal cornea through which a microelectrode was inserted into the proximal layer of the retina.

Monochromatic light was provided by a 500 W Xenon arc lamp together with a set of 22 narrow band interference filters with maxima ranging from 290 to 700 nm. The light intensity was attenuated with neutral density filters and an optical wedge over a range of 4 log units. The light beam was focused on the tip of an optical fiber that led the light into the cage. The other end of the optical fiber was attached to a Cardan arm perimeter device. The resulting stimulus approximated a point source of light (1.6° in diameter) which was adjusted to the optical axis of the impaled photoreceptors. The maximal quantum flux of each unpolarized monochromatic light was adjusted to about 5.0×10^{11} photons · cm⁻² · sec⁻¹ at the corneal surface. The stimulus was a 30 ms light pulse.

After impalement, first the angular position of the ommatidial optical axis at which the photoreceptor responded maximally was determined. The position of the optical axis was recorded as two values of angles read from the horizontal and the vertical goniometers attached to the perimeter device. We then recorded the responses of the photoreceptor to a series of unpolarized monochromatic flashes. The stimulus intensity-response (V-log I) function was recorded at the peak wavelength (λ_{\max}) of the impaled photoreceptor, also with unpolarized flashes. Only when the maximal response amplitude (V_{\max}) exceeded 40 mV, did we record the responses to polarized light at the λ_{\max} with an intensity that elicits around 50% of V_{\max} . The *e*-vector orientation (ϕ) was adjusted by rotating the UV-transparent polarization filter (HHP'B, Polaroid) in front of the tip of the optical fiber. The *e*-vector orientation was initially set parallel to the animal's dorso-ventral axis: this angle was defined as 0° and the animal's anterior side as 90°. A set of 36 responses to polarized light flashes at 10° interval was recorded so as to make the latter half of the recording as a repetition of the first half.

The two responses to each *e*-vector angle, thus obtained were averaged.

The spectral and polarization response amplitudes were converted into sensitivity by using the photoreceptor's V-log I function as a gauge function, i.e. to calculate the photon numbers required for a criterion response. The reciprocal of the photon number was then plotted as sensitivity, and the resulting curve was normalized. The V-log I function was drawn by fitting the data to the Naka-Rushton equation, $V/V_{\max} = I^n/(I^n + K^n)$, where *I* = stimulus intensity, *V* = response amplitude, V_{\max} = maximum response amplitude, and *K* = stimulus intensity eliciting 50% V_{\max} . The exponent *n* of the investigated receptors appeared to be constant ($n = 0.75 \pm 0.11$; mean ± SD). The *e*-vector orientation to which the polarization sensitivity curve expresses its peak (ϕ_{peak}), and the polarization sensitivity (PS = maximal sensitivity / minimal sensitivity) were determined from the sinusoidal curve fitted to the data using the least squares method.

Results

Recorded region

We recorded the spectral and polarization sensitivities from 109 photoreceptors in the middle part of the left eye of *Papilio xuthus*. Each asterisk in Fig. 1 represents the localization of the optical axis of the recorded photoreceptor. Most of the photoreceptors were confined to this lateral looking eye region.

Arrangement of ommatidia in the lateral looking eye region

An ommatidium in the lateral looking eye region contains nine photoreceptors (Fig. 2). Four distal photoreceptors (R1-4) bear microvilli in the distal tier of the

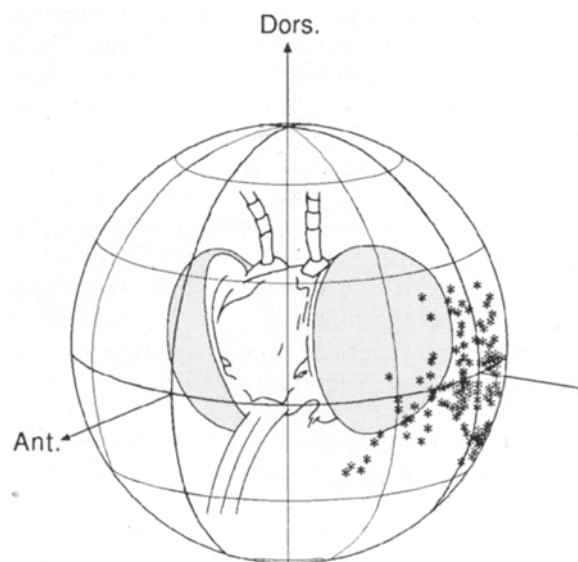


Fig. 1 Localization of the optical axes of 109 recorded photoreceptors. Each asterisk corresponds to one photoreceptor. The recorded photoreceptors were confined to the lateral looking eye region. *Ant.*, anterior; *Dors.*, dorsal

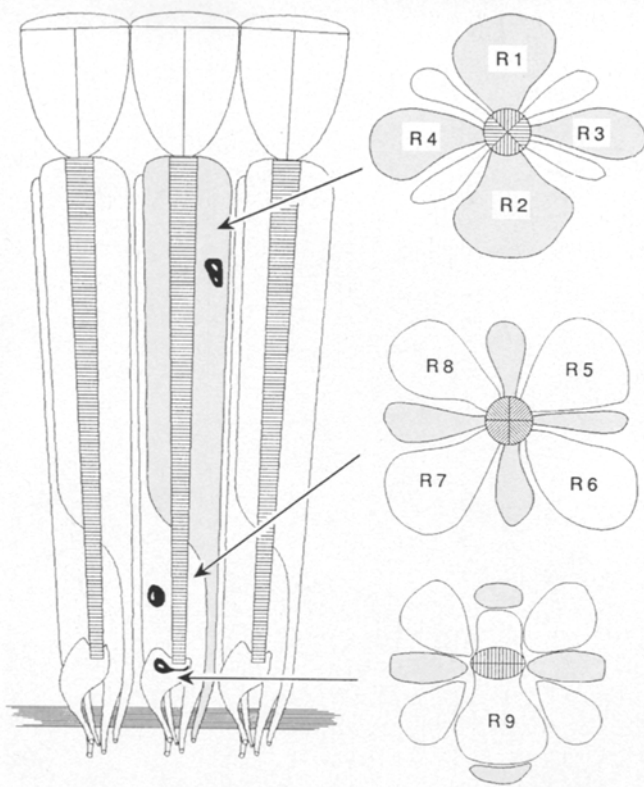


Fig. 2 Schematic representation of *Papilio* ommatidia. The fused rhabdom is tiered. The distal tier is made up of the microvilli of four distal photoreceptors (R1-4). The others (R5-9) construct the proximal tier; the bilobed R9 contributes only at the base of the rhabdom

rhabdom. These microvilli are parallel to the dorso-ventral (R1, 2) or antero-posterior (R3, 4) axes. The proximal tier of the rhabdom consists of the diagonally oriented microvilli from four proximal photoreceptors (R5-8) and the dorso-ventrally oriented microvilli from the basal photoreceptor (R9).

To determine whether or not the ommatidia of *Papilio* are twisted about the longitudinal axis, we carefully investigated the arrangement of ommatidia in light microscopic sections. Figure 3a shows a horizontal section roughly through the equator. The line indicates the cut plane of the oblique section shown in Fig. 3b. For each ommatidium in Fig. 3b, the relative position of R1 to R2 was determined by drawing a line between cell bodies of these photoreceptors: the line thus indicates the "symmetry-axis" of a given ommatidium (Fig. 3c). It appeared that the axes are quite uniformly oriented with very little distortion: there is no clear sign of ommatidial twist.

The cell bodies of R5-8 occupy the diagonal positions in the ommatidium, but the microvillar orientations were not exactly diagonal. Unlike R1 and R2 whose microvilli curve (Bandai et al. 1992), R5-8 have straight and parallel microvilli. We measured the microvillar angles of R5-8 in 10 ommatidia in EM

transverse sections at the level where the rhabdom consists exclusively of microvilli from R5-8. The angle formed by the eye's dorso-ventral axis and a microvillus was measured for at least 5 microvilli in each rhabdomere. R6 and R8 appeared to have microvilli oriented at around 39° . The microvilli of R5 and R7 are oriented at around 144° (Table 1).

Distribution of the peak angle ϕ of the polarization sensitivity

The purpose of this study was to reveal the spectral properties of the proximal and basal photoreceptors. We therefore placed the electrode into the proximal tier of the retina, and recorded spectral and polarization sensitivities of the impaled photoreceptors.

Figure 4 shows the distribution histogram of the polarization peak angles (ϕ_{peak}) (bin width = 10°). The histogram represents three bands at around 0° , 40° , and 150° . No cell had a ϕ_{peak} at around 90° . The ϕ_{peak} of a given photoreceptor is expected to be identical to the orientation of the microvillar longitudinal axis (Moody and Parriss 1961), as found previously for the distal receptors in *Papilio xuthus* (Bandai et al. 1992). Therefore, the photoreceptors with peak angle at around 40° correspond to R6 or R8 whose microvilli are oriented at 39° on average (Table 1). Similarly, the cells that peak at around 150° are either R5 or R7. And, the PS of R9 should peak at around 0° .

There seem to be also photoreceptors whose ϕ_{peak} cannot be simply explained by the microvillar angles of proximal rhabdomeres (e.g. the columns of $10 \sim 30^\circ$, $160 \sim 170^\circ$ etc. in Fig. 4). Presently we attribute the discrepancy to experimental error, such as mechanical distortion produced by the impaled electrode, rather than to unknown photoreceptor types whose microvillar angles match to these ϕ_{peak} .

The PS varied between 1.5 and 10.1; the average PS was 2.0 ± 1.2 (mean \pm SD).

Spectral sensitivities

Figure 4 also represents the spectral type of the proximal and basal photoreceptors. The recorded spectral types were only green and red. Seventy six out of 109 photoreceptors were of the red type: we did not encounter the UV, violet, and blue types that were identified in the *Papilio* distal retina (Arikawa et al. 1987; Bandai et al. 1992). The relative contents of red receptors in each group of photoreceptors with different ϕ are summarized in Table 2. Ten out of 13 photoreceptors (77%) of $\phi_{\text{peak}} = 30$ to 50° (single asterisk in Fig. 5) and 20 out of 27 photoreceptors (74%) of $\phi_{\text{peak}} = 140$ to 160° (double asterisks) were of the red type. Among 27 photoreceptors of $\phi_{\text{peak}} = 170$ to 10° (triple asterisks in Fig. 5), 13 (48%) were of the red type.

Fig. 3 **a** Horizontal section of left eye through the equator. The *line* indicates the cut plane of the section shown in **b**. **b** Oblique section through the *line* drawn in **a**. Ommatidial transverse sections at the distal tier (*left*), proximal tier (*right*), and the basement membrane (*BM*) are seen. **c** Traced R1-2 axes of all ommatidia in the oblique section. The *numbers* and *arrows* below indicate the relative depth of the section from the corneal surface. *ANT*, anterior; *BM*, basement membrane; *L*, lamina; *M*, medulla; *R*, retina. Scale bars = 500 μm (**a**), 100 μm (**b**)

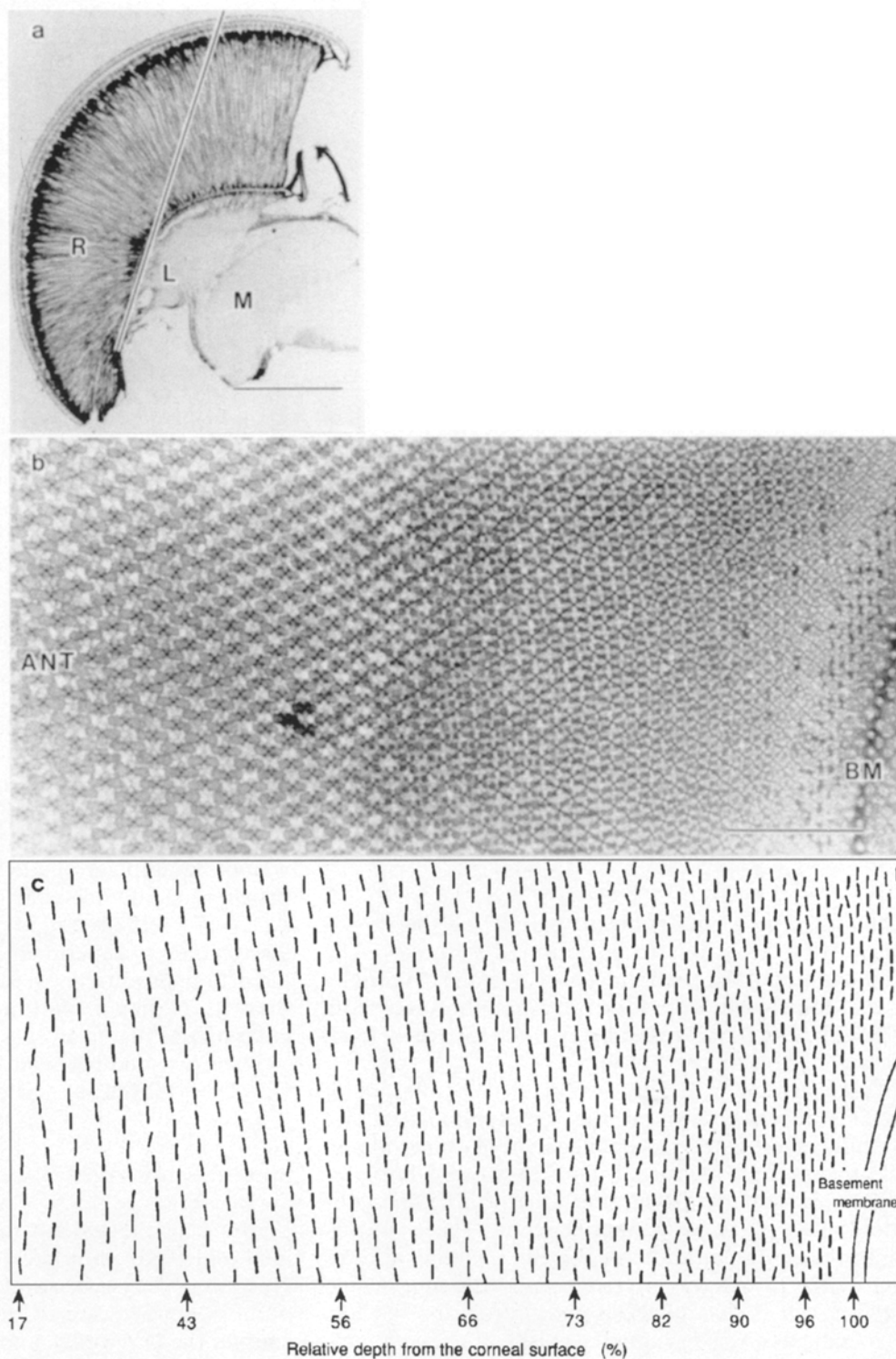


Figure 5 shows the spectral sensitivity curves. Figure 5a demonstrates the average sensitivity curves of all (33 green and 76 red) photoreceptors. Figure 5b presents the averaged spectral sensitivity curves of each photoreceptor group with different ϕ_{peak} . Among red

receptors, those with polarization sensitivity peaking between 170° and 10° have a reduced spectral sensitivity in the wavelength range of 420 to 460 nm (single arrow). In green receptors, spectral sensitivity in the red appears to be correlated with ϕ_{peak} (double arrow).

Table 1 Microvillar orientation of proximal photoreceptors R5-8

| Cell type | Microvillar angle (degrees, mean \pm SD) |
|-----------|-----------------------------------------------|
| R6/8 | 38.9 \pm 5.8 |
| R5/7 | 144.3 \pm 11.2 |

The angles formed by the animal's dorso-ventral axis and the microvilli were measured on EM transverse sections of proximal rhabdoms. Ten ommatidia were selected for the measurements ($n = 10$)

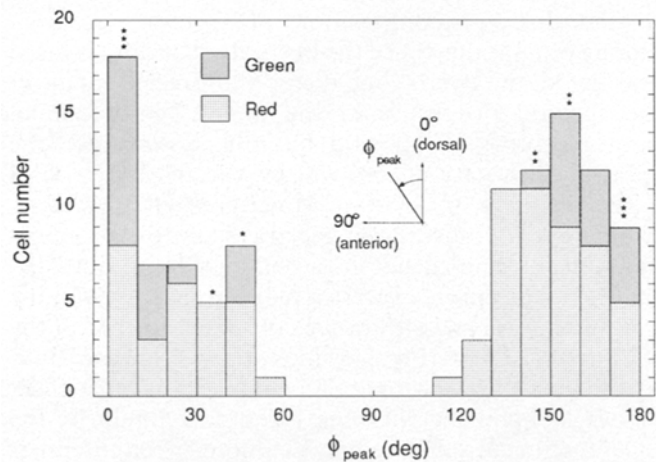


Fig. 4 Stack histogram showing the distribution of ϕ_{peak} of all 109 photoreceptors recorded in the present study. Spectral type of photoreceptors was determined by the peak wavelength of the spectral sensitivity. Columns with asterisks correspond to the cells mentioned in Fig. 5b and Table 2. The dorso-ventral axis and the anterior side were defined as 0° and 90° , respectively (inset). Note that $0^\circ = 180^\circ$

Table 2 Spectral types of 67 out of 109 photoreceptors whose ϕ_{peak} fell into three particular angle ranges

| ϕ_{peak} range (degrees) | Green | Red | Total | Red % | Expected cell type |
|--------------------------------------|-------|-----|-------|-------|--------------------|
| *30 ~ 50 | 3 | 10 | 13 | 76.9 | R6 or R8 |
| **140 ~ 160 | 7 | 20 | 27 | 74.1 | R5 or R7 |
| ***170 ~ 10 | 14 | 13 | 27 | 48.1 | R9 |

The ϕ_{peak} of the other 42 photoreceptors peak somewhere in between. Asterisks indicate the columns in Fig. 4 from which the data were taken. The spectral sensitivity of each category is shown in Fig. 5b

Discussion

The ommatidia of *Papilio* are not twisted

In the previous study, where we first applied the polarization method to the distal tier (Bandai et al. 1992), we injected lucifer yellow into the photoreceptors after recording. The direction of the microvilli of the stained

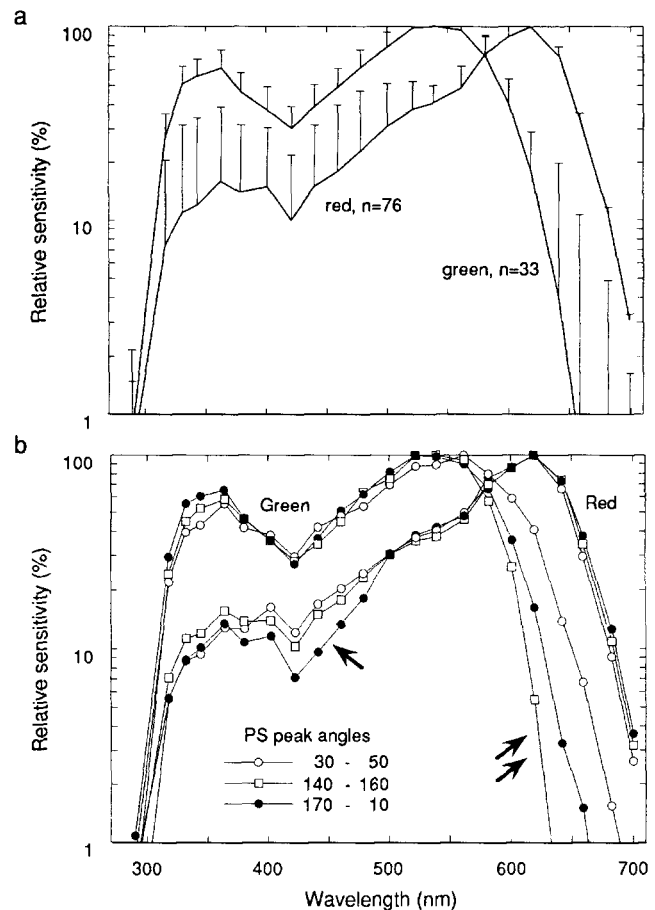


Fig. 5a, b Spectral sensitivity curves. **a** Mean (\pm SD) spectral sensitivity curves of green ($n = 33$) and red ($n = 76$) receptors. **b** Averaged spectral sensitivity curves of green and red receptors categorized by the PS peak angles: ϕ_{peak} at $30 \sim 50^\circ$ (open circle, single asterisk in Fig. 4), at $140 \sim 160^\circ$ (open square, double asterisks), and at $170 \sim 10^\circ$ (filled circle, triple asterisks). Standard deviations were not shown for clarity. The photoreceptors appearing in **b** are the ones described in Table 2. For arrows, see text

cell always corresponded with the ϕ_{peak} of the cell's polarization sensitivity, providing further evidence for the view that the ommatidia of *Papilio xuthus* do not twist. The histology presented here demonstrates that the proximal ommatidia are not twisted either.

The twist, occurring in the ommatidia of several insects, significantly reduces the PS, and thus has been thought to prevent confusion between polarization and color differences such as those from the waxy surfaces of leaves (Wehner and Bernard 1993). The rhabdomeral microvilli of some, but not all, distal photoreceptors of *Papilio* actually curve in different directions depending on the depth in the ommatidium (Bandai et al. 1992). Distal photoreceptors with curved microvilli were also reported for pierid (Kolb 1978) and nymphalid butterflies (Gordon 1977; Kolb 1985). In fact, we sometimes encountered distal photoreceptors without clear PS in *Papilio xuthus* and also in a nymphalid species *Sasakia charonda* (Arikawa, in preparation), which presumably

were photoreceptors with curved microvilli. Such an organization of microvilli might be an alternative strategy, taken by butterflies, to solve the false-color problem.

Localization of spectral receptors in the ommatidium

We classified the photoreceptors with $\phi_{\text{peak}} = 0^\circ$ as R9, the basal photoreceptor, although such a ϕ_{peak} can also be recorded from R1 or R2. In fact, cells with $\phi_{\text{peak}} = 0^\circ$ were frequently impaled when the electrode was placed in the distal tier (Bandai et al. 1992). These photoreceptors must be either R1 or R2, for R9 does not have any apparent process in the distal tier, and thus has very little chance to be impaled. The spectral type of R1 and R2 was UV, violet, or blue (Fig. 6). On the other hand, the photoreceptors with ϕ_{peak} at 0° that we encountered throughout this work were all green or red type. All green receptors in the distal tier were R3 or R4, whose $\phi_{\text{peak}} = 90^\circ$. This means that those green receptors that have their ϕ_{peak} at 0° should be R9, as they bear microvilli parallel to the dorso-ventral axis.

Figure 6 summarizes the localization of spectral receptors in the *Papilio* ommatidium. 75% of the recorded R5-8 and 48% of the recorded R9 were of the red type (Table 2). Since the cross-sectional areas of R5-8 are almost equal at least in the lateral looking eye region (Fig. 3), the relative number of recording most likely reflects the relative number of spectral types; i.e.

75% of R5-8 are of the red type. Similarly, in this region of the compound eye, the size of R9 is almost the same in all ommatidia, which indicates that 48% of ommatidia have R9 of the red type.

The results indicate that not all ommatidia are identical in terms of the content of spectral receptor types (Fig. 6). It follows that a single ommatidium can contain at the minimum two (e.g. R1-2 = UV, R3-9 = green), and maximally four (e.g. R1 = UV, R2 = blue, R3-4 = green, R5-9 = red) types of spectral receptors.

The rather large standard deviation observed in the spectral sensitivity functions (Fig. 5a) is probably due to the different composition of spectral receptors among ommatidia. Since the butterfly rhabdom is fused and tiered, the overlaying, distal photoreceptors affect the spectral properties of the underlying, proximal photoreceptors by spectral filtering. Specifically, the spectral sensitivity of R9s will be affected by those of R5-8, which themselves are already affected by R1-4. A different composition of spectral receptors produces different filtering effects in the ommatidium. Actually, the R9 red receptors express a reduced sensitivity in the 420-460 nm wavelength range compared to that of the R5-8 red receptors (Fig. 5b, single arrow). This sensitivity difference may be due to an enhanced filtering effect of overlaying violet or blue receptors. Similarly, the difference in cut-off wavelengths among green receptors (Fig. 5b, double arrow) may be the result of variable lateral filtering, especially by the red screening pigment in the cell body of R5-8 (Ribi 1987; Snyder et al. 1973). Obviously, before a detailed quantitative evaluation of filtering effects can be given, precise knowledge of the composition of spectral types within an ommatidium is necessary.

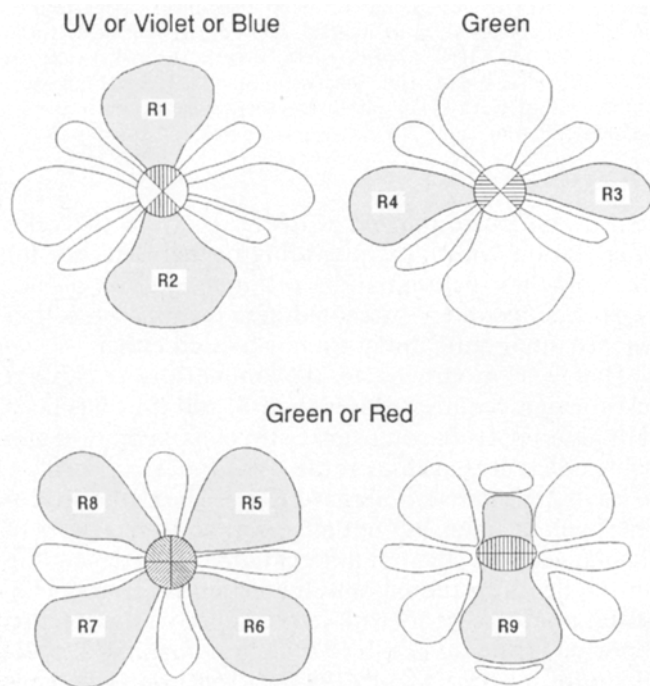


Fig. 6 Schematic representation of spectral receptor localization in the ommatidium of *Papilio*. The spectral type of distal photoreceptors (R1-4) have been identified previously (Bandai et al. 1992)

Possible color vision of the butterfly

Although real color vision, involving learning, has been demonstrated only in primates and honeybees (Goldsmith 1990), the hypothesis of color vision in brightly colored butterflies is irresistible. Based on anatomy, Strausfeld and Lee (1991) suggested that in flies the input of wavelength information is mediated by the central photoreceptors (R7 and R8), whose axons extend directly into the medulla, the second optic ganglion. Recent behavioral work on blowflies (Troje 1993) suggests that wavelength discrimination is mediated by two pairs of central photoreceptors R7 and R8, forming a wavelength opponent system. In the Australian orchard butterfly *Papilio aegaeus*, R1, R2, and R9 are the long visual fibers (Ribi 1987). We know that in *Papilio xuthus* R1 and R2 are of either UV, violet, or blue receptors, whereas R9s are green or red receptors. Assuming that the axons of R1, R2, and R9 are also long visual fibers in *Papilio xuthus*, these fibers include a complete set of five spectral receptors (Fig. 6). Therefore, if the central visual pathway supplied by the long

visual fibers processes wavelength information, color vision of *Papilio xuthus*, if any, could be pentachromatic. Obviously, direct evidence for the presence of color vision has to await further behavioral analysis.

Acknowledgements We thank Drs. D.G. Stavenga and E. Eguchi for critical reading of the manuscript. We also thank Ms Michiyo Kinoshita for providing Fig. 3a. This work was supported by grants from the Whitehall Foundation and from the Ministry of Education, Science, and Culture of Japan to K. Arikawa.

References

- Arikawa K, Inokuma K, Eguchi E (1987) Pentachromatic visual system in a butterfly. *Naturwissenschaften* 74: 297–298
- Bandai K, Arikawa K, Eguchi E (1992) Localization of spectral receptors in the ommatidium of butterfly compound eye determined by polarization sensitivity. *J Comp Physiol A* 171: 289–297
- Cronin TW, Marshall NJ (1989) A retina with at least ten spectral types of photoreceptors in a mantis shrimp. *Nature* 339: 137–140
- Goldsmith TH (1990) Optimization, constraint, and history in the evolution of eyes. *Q Rev Biol* 65: 281–322
- Gordon WC (1977) Microvillar orientation in the retina of the nymphalid butterfly. *Z Naturforsch* 32c: 662–664
- Kolb G (1978) Zur Rhabdomstruktur des Auges von *Pieris brassicae* L. (Insecta, Lepidoptera). *Zoomorphologie* 91: 191–200
- Kolb G (1985) Ultrastructure and adaptation in the retina of *Aglais urticae* (Lepidoptera). *Zoomorphologie* 105: 90–98
- Moody MF, Parriss JR (1961) The discrimination of polarized light by *Octopus*: a behavioral and morphological study. *Z Vergl Physiol* 44: 268–291
- Ribi WA (1987) Anatomical identification of spectral receptor types in the retina and lamina of the Australian orchard butterfly, *Papilio aegaeus aegaeus* D. *Cell Tissue Res* 247: 49–59
- Shimohigashi M, Tominaga Y (1991) Identification of UV, green and red receptors, and their projection to lamina in the cabbage butterfly, *Pieris rapae*. *Cell Tissue Res* 247: 49–59
- Snyder AW, Menzel R, Laughlin SB (1973) Structure and function of the fused rhabdom. *J Comp Physiol* 87:99–135
- Strausfeld NJ, Lee J-K (1991) Neuronal basis for parallel visual processing in the fly. *Visual Neurosci* 7: 13–33
- Troje N (1993) Spectral categories in the learning behaviour of blowflies. *Z Naturforsch C* 48: 96–104
- Wehner R, Bernard GD (1993) Photoreceptor twist - a solution to the false-color problem. *Proc Natl Acad Sci USA* 90: 4132–4135
- Yang EC, Osorio D (1991) Spectral sensitivities of photoreceptors and lamina monopolar cells in the dragonfly, *Hemicordulia tau*. *J Comp Physiol A* 169: 663–669